Spin Physics at ANKE-COSY

S. Dymov[a,b] for the ANKE collaboration

[a] *Universität Erlangen-Nürnberg, 91058 Erlangen, Germany*
[b] *Joint Institute for Nuclear Research, 141980 Dubna, Russia*

The COSY accelerator (Jülich, Germany) provides beams of polarized protons and deuterons. The ANKE facility at COSY is equipped with polarized hydrogen and deuterium atomic gas targets. The reactions investigated with polarized probes at ANKE include the deuteron break-up at small and large momentum transfer, the pion production processes in pp and pn collisions and the near-threshold η meson production in $\vec{d}p \to {}^3He\eta$ process. Use of the polarized proton beam properties allowed for a precision measurement of the η meson mass.

The future experimental program covers the study of the elementary pp and pn-interaction with polarized beams up to the maximal COSY energy, and a double polarized measurement of the $A_{x,z}$ spin correlation parameter in the $pN \to \{pp\}_s\pi$ process.

1. Introduction

The Cooler Synchrotron and storage ring COSY provides beams of polarized protons and deuterons in the 0.3–3.7 GeV/c momentum range. The ANKE [1] facility, an internal magnetic spectrometer at COSY, is equipped with polarized internal hydrogen and deuterium atomic gas targets [2]. Both vector and tensor polarizations are available for the deuteron COSY beam as well as for the ANKE deuterium target. Until now, only transverse polarizations of the beam and target were available, but the installation of a Siberian snake at COSY, foreseen in 2013, will provide the longitudinally polarized proton beam option.

These features allow to study various hadronic processes in the intermediate energy range in single and double polarization experiments [3, 4].

The reactions investigated at ANKE include: the **charge-exchange deuteron break-up** (CE) (access to the elementary CE pn scattering amplitudes) [5, 6], the **cumulative mesonless deuteron break-up** (study of short-range NN interactions) [7] and **pion production processes in pp and pn collisions** in the near-threshold region (information on the contact $NN\pi$ interaction in the Chiral perturbation theory) [8, 9] as well as in the $\Delta(1232)$ production region (test of existing phenomenological models of $NN \to NN\pi$ process) [10]. These reactions are considered in a kinematical condition, where "diproton" $\{pp\}_s$, e.g. a proton pair with the low excitation energy, is produced in the final state. The ANKE spectrometer is particularly well-suited for this kinematics.

The presence of the tensor polarized deuteron beam lets us investigate the **spin dependence of the $\vec{d}p \to {}^3He\eta$ excitation function** near the η production threshold [11]. This study covers the questions of the η-nucleon force, the η-nucleus final-state interaction (FSI) and threshold enhancement, and possible existence of quasi-bound η-nucleus states.

Another study at ANKE utilises the fact, that in experiments with polarised deuteron beams at a storage ring, the beam momentum can be determined very precisely through the study of artificially induced depolarising resonances [12]. This led to a **determination of the mass of the η meson** that is as precise as any other in the literature [13].

Below we present the latest results of the ANKE programs on the near-threshold pion production and the elementary NN interaction.

2. The near-threshold single pion production

The ANKE experimental programme on the near-threshold pion production aims to measure the cross sections and spin observables in the $pp \to \{pp\}_s\pi^0$ and $np \to \{pp\}_s\pi^-$ reactions [14, 15]. The symbol $\{pp\}_s$ here denotes a diproton, that is, an unbound proton pair with a very low excitation energy, $E_{pp} < 3$ MeV. The selection of a low excitation energy ensures the dominance of the $^1S_0$ state of the diproton, which simplifies significantly the theoretical analysis. A full data set of all observables at low beam energies would allow us to determine the partial wave amplitudes which, in turn, would provide a non-trivial test of chiral perturbation theory [16] and also lead to the determination of the value of the parameter d, which represents the important contact term that affects the pion p-wave amplitudes.

The types of experiments, possible for both π^0 and π^- production, are the measurement of $d\sigma/d\Omega$, the beam or target analysing power A_y, the in-plane spin-correlation $A_{x,x}$, and the mixed correlation parameter $A_{x,z}$.

At low energies it is reasonable to assume that data can be analysed by truncating the partial wave expansion at orbital angular momentum $\ell = 2$. It is shown in [17] that the magnitude of one of the p-wave amplitudes is then fixed completely by the measurement of $(1 - A_{x,x}) \cdot d\sigma/d\Omega$ for $np \to \{pp\}_s\pi^-$ and that the magnitude of the other p-wave amplitude and its relative phase can be deduced from a combined analysis of this with our cross section and analysing power data for $pp \to \{pp\}_s\pi^0$and $np \to \{pp\}_s\pi^-$. These data will provide two determinations of the LEC d. Measurements of the mixed spin-correlation parameters $A_{z,x}$ are not required for the extraction of the p-wave amplitudes, though such information is vital in order to identify the d-wave terms.

2.1. Measurement of cross section and analysing power. As first steps in the programme, measurements with a polarised proton beam incident on unpolarised hydrogen and deuterium cluster targets were performed at a beam energy of $T_p = 353$ MeV [14, 15]. The beam polarisation and the luminosity were both estimated from the data on the $\vec{p}p \to d\pi^+$ and $\vec{p}p \to pp$ processes in the pp-case, and the quasi-free $\vec{p}n \to d\pi^0$ in the pd-case, that were taken in parallel.

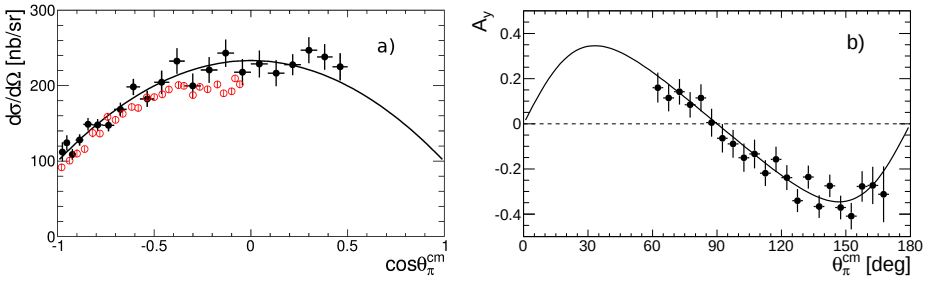

Fig. 1. (**a**) Differential cross section for the $pp \to \{pp\}_s\pi^0$ reaction at 353 MeV as a function of the cosine of the pion center-of-mass angle. Solid (black) circles represent ANKE measurements [8]. Open (red) circles are CELSIUS data obtained at 360 MeV [18]. (**b**) Measured values of A_y for the $\vec{p}p \to \{pp\}_s\pi^0$ reaction [8]. The curves in both plots are results of the partial wave analysis of ANKE data.

The ANKE results for the differential cross section and the vector analysing power for the $pp \to \{pp\}_s\pi^0$ reaction are shown in Figs. 1. For a spin-singlet diproton, the spin structure of the $pp \to \{pp\}_s\pi^0$ or $np \to \{pp\}_s\pi^-$ reaction is that of $\frac{1}{2}^+\frac{1}{2}^+ \to 0^+0^-$. For the $pp \to \{pp\}_s\pi^0$ reaction, only even pion partial waves are allowed. If one considers only pion waves with $l \leq 2$, a non-zero value of the analysing power in this process must arise from the interference between the s and d waves. The strong A_y signal demonstrates the importance of this interference.

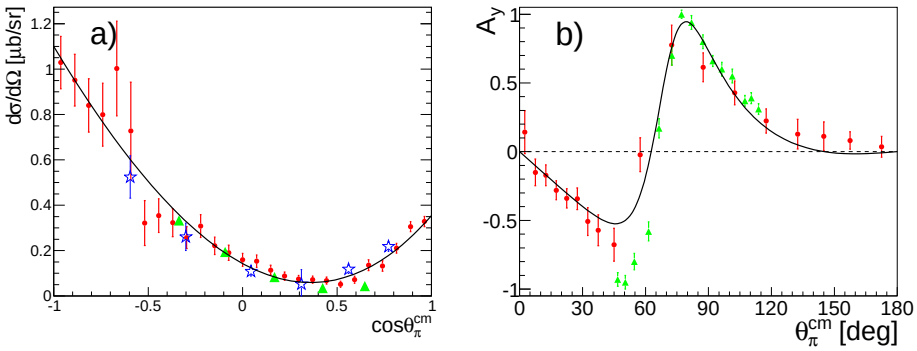

Fig. 2. (**a**) Unpolarised differential cross section for the $pn \to \{pp\}_s\pi^-$ reaction at $\approx$ 353 MeV. The ANKE data [9] are shown by red circles and the TRIUMF results [19] by green triangles. The arbitrarily scaled TRIUMF cross sections extracted from $\pi^{-3}\mathrm{He} \to pnp_{\mathrm{spec}}$ data [20] are also included (blue stars). (**b**) Measured values of A_y for the $\vec{p}n \to \{pp\}_s\pi^-$ reaction showing both the ANKE (circles) [9] and TRIUMF data [21] (triangles). The solid curves in both plots are partial wave fits to ANKE data.

The results for the differential cross-section and the analysing power of the $\vec{p}n \to \{pp\}_s\pi^-$ reaction [9] are displayed in Fig. 2. Whereas the TRIUMF results only cover the central region of pion angles [19], the ANKE data [9] in Fig 2 extend over the whole angular domain. The two data sets are consistent in the backward hemisphere but the TRIUMF measurements show no indication of the rise at forward angles that is seen at ANKE. Some confirmation of the ANKE angular shape is offered by pion absorption data, $\pi^{-3}\mathrm{He} \to pnp_{\mathrm{spec}}$, where the unobserved slow proton is assumed to be a spectator [20]. In this case the reaction can be interpreted as being $\pi^-\{pp\}_s \to pn$, though the internal structure of the bound diproton is very different to that in the production data. The forward/backward peaking is in complete contrast to the results found for π^0 production [18] and is an indication of the dominance of the $I = 0$ p-wave amplitudes in this reaction.

The agreement with the TRIUMF A_y data [21] is good in the backward hemisphere and both show a strong and rather asymmetric fluctuation in the central angular region.

Keeping terms up to pion d waves, the $pp \to \{pp\}_s\pi^0$ data at 353 MeV [8] can be parameterised in terms of the three partial wave amplitudes M_s^P, M_d^P, and M_d^F, corresponding to the transitions, ${}^3P_0 \to {}^1S_0s$, ${}^3P_2 \to {}^1S_0d$, and ${}^3F_2 \to {}^1S_0d$, respectively. In proton-neutron collisions there are also the two p-wave transitions, ${}^3S_1 \to {}^1S_0p$ and ${}^3D_1 \to {}^1S_0p$ that arise in the isospin $I = 0$ case, and for these we introduce amplitudes M_p^S and M_p^D, respectively. The cross section and analysing power data are insufficient to perform a full amplitude analysis without further assumptions. These were to neglect the coupling between the initial ${}^3P_2$ and ${}^3F_2$ waves and to use the Watson theorem to determine the phases of the production amplitudes from these

and also the $^3P_0$ wave. There are then seven real parameters available to describe essentially ten features in Figs. 1 and 2. The success achieved here suggests that the phase assumptions are basically correct. The analysis shows that d-wave production is confined almost purely to the $^3P_2$ channel but by far the largest term is associated with p-wave production from the initial $^3D_1$ state.

2.2. Measurement of $A_{x,x}$ and $A_{y,y}$ in $\vec{n}\vec{p} \to \{pp\}_s\pi^-$ The spin-correlation coefficients $A_{x,x}$ and $A_{y,y}$ of the quasi-free $\vec{n}\vec{p} \to \{pp\}_s\pi^-$ reaction were measured at ANKE in 2011 by using the vector polarised deuteron beam and the hydrogen polarised target, equipped with a long storage cell [22]. The main source of background in this measurement was the interaction of a beam particles with the aluminum storage cell walls. In order to obtain the shape of the background in the missing mass spectra, a dedicated measurement was made with the N_2 gas in the storage cell.

The $A_{y,y}$ results are shown in Fig. 3 in terms of the pion emission angle. As expected, $A_{y,y}$ is consistent with unity over the whole angular range. To reduce the uncertainty in the extraction of $A_{x,x}$, it was assumed that $A_{y,y} = 1$ and the analysis repeated, leading to the results shown in Fig. 4.

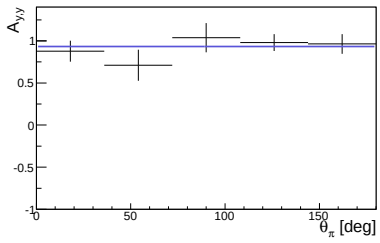

Fig. 3. The spin-correlation coefficient $A_{y,y}$ for the $\vec{n}\vec{p} \to \{pp\}_s\pi^-$ reaction measured at 353 MeV (preliminary).

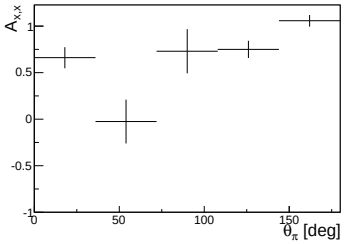

Fig. 4. The spin-correlation coefficient $A_{x,x}$ for the $\vec{n}\vec{p} \to \{pp\}_s\pi^-$ reaction measured at 353 MeV (preliminary).

For the $np \to \{pp\}_s\pi^-$process, $(1 - A_{x,x}) \cdot d\sigma/d\Omega \sim |\delta|^2 \sin^2\vartheta_\pi$, where $|\delta|^2$ is the square of one of the p-wave production amplitudes that is linked to the $4N\pi$ contact interaction [17]. The differential cross section and the preliminary spin-correlation data give $(1 - A_{x,x}) \cdot d\sigma/d\Omega(90^\circ) = (96 \pm 25)$ nb/sr. This is consistent with the results of the partial wave analysis [9], which predicts a value of 52 nb/sr.

3. The nucleon-nucleon programme

A good understanding of the NN interaction still remains one of the principal goals of nuclear and hadronic physics. Apart from their intrinsic importance for the study of nuclear forces, NN elastic scattering data are also necessary ingredients in the modeling of meson production and other nuclear reactions at intermediate energies.

A great effort has been made at ANKE in the study of the spin-dependent terms in large angle neutron-proton scattering. It was pointed out that the $dp \to \{pp\}_s n$ charge exchange at small angles was very sensitive to the spin-spin terms in the $np \to pn$ amplitude provided the excitation energy E_{pp} in the final pp system was kept low [23]. Under such conditions the

$\{pp\}_s$ is in a $^1S_0$ state and the charge exchange necessarily involves a spin flip from the initial np spin-triplet of the deuteron. Furthermore, measurements of the deuteron tensor analysing powers A_{xx} and A_{yy} allow one to distinguish between the contributions from the three spin-spin np amplitudes.

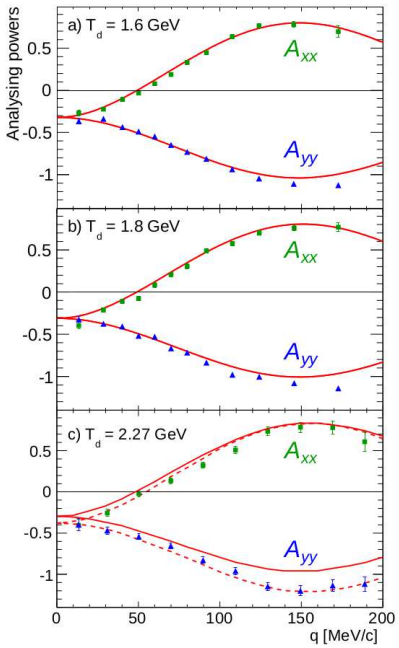

Fig. 5. Cartesian deuteron analysing powers for the $dp \to \{pp\}_s n$ reaction at T_d = 1.2, 1.6, and 1.8 GeV [6]. The impulse approximation predictions [24] have been evaluated with the SAID amplitudes [25] (solid curves) and also, at the highest energy, when the longitudinal spin- spin amplitude is scaled by a factor of 0.75.

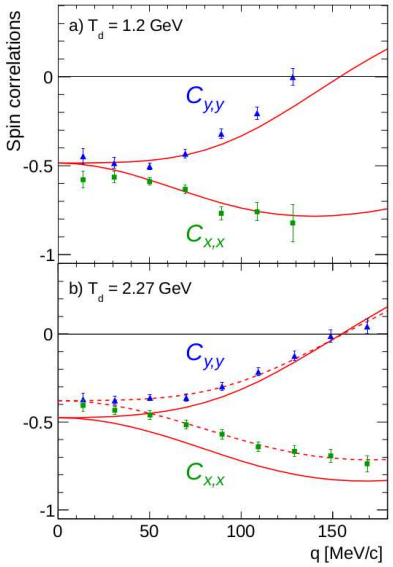

Fig. 6. Transverse spin correlation parameters in the $dp \to \{pp\}_s n$ reaction at (a) 1.2 and (b) 2.27 GeV compared to the predictions of an impulse approximation model (solid curves). Better agreement is found at the higher energy if the longitudinal input is scaled by a factor of 0.75 (dashed curves).

Measurements were carried out at Saclay [26, 27] but only in regions where the NN amplitudes were reasonably well known. These have been extended in fine steps in momentum transfer q to higher energy at ANKE [5, 6]. The ANKE analysing power results at 1.6, 1.8, and 2.27 GeV are compared in Fig. 5 to these impulse approximation predictions using up-to-date np amplitudes [25] as input. The satisfactory agreement at the two lower energies, and also in the values of the differential cross sections, shows that the theoretical description is adequate here.

Above about 1 GeV np data become rather sparse. It comes therefore as no surprise that, when the same approach is employed on the higher energy data shown in Fig. 5, the current SAID amplitudes [25] give a poor overall description of the results. However, if the longitudinal spin-spin amplitude is multiplied by a global factor of 0.75, the agreement is much more satisfactory. This is evidence that the charge exchange data can provide useful input to the NN database.

Confirmation of these conclusions is to be found in the measurements of the deuteron-proton spin correlation parameters measured with the polarised hydrogen gas cell. Results on this are shown in Fig. 6. In impulse approximation, these are sensitive to the interference between the longitudinal spin-spin amplitude and the two transverse ones. Whereas there is satisfactory agreement with the theoretical predictions at 1.2 GeV, the model is much more satisfactory at 2.27 GeV if the longitudinal input is scaled by a factor of 0.75.

In addition to measuring the spin correlations with the polarised cell, data were also obtained on the proton analysing power in the $\vec{d}p \rightarrow \{pp\}_s n$ reaction. The message here is very similar to that for the other observables. At 600 MeV per nucleon the SAID input reproduces the experimental points very well but it seems that at 1135 MeV the SAID description of the spin-orbit amplitude has serious deficiencies.

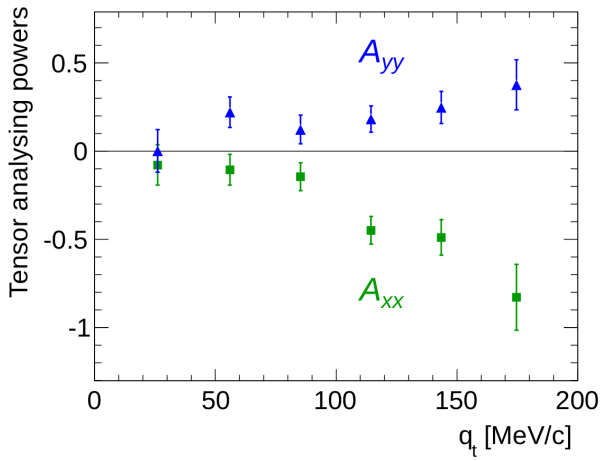

Fig. 7. Tensor analysing powers for the $\vec{d}p \rightarrow \{pp\}_s X$ reaction at 2.27 GeV as a function of the transverse momentum transfer. The data are integrated over the mass range $1.19 < M_X < 1.35$ GeV/c^2 [28].

As well as studying the $\vec{d}p \rightarrow \{pp\}_s X$ data to extract the neutron as a missing-mass peak, results were also obtained where $m_X > m_N + m_\pi$. These events must be associated with pion production, especially through the Δ isobar. The first indications shown in Fig. 7 are that the Cartesian analysing powers are largely opposite in sign to those for $\vec{d}p \rightarrow \{pp\}_s n$. These data will therefore yield information on the amplitude structure of the $NN \rightarrow N\Delta$ reaction.

4. Outlook

Although the partial wave description of the pion production data is both plausible and impressive, one needs to measure other types of observables in order to test its validity. The preliminary results on the transverse spin-spin correlation in the $\vec{n}\vec{p} \rightarrow \{pp\}_s \pi^-$ reaction are consistent with the predictions of the amplitude analysis discussed in Sec. 2. Further checks could be made through measurements of the longitudinal-transverse spin correlation but these will require the installation of a Siberian snake to rotate the proton spin. This should take place early in 2013.

The snake will also allow us to study the spin-correlation parameter A_{00kn} in small angle pp elastic scattering. Though the charge exchange programme with a polarised deuteron beam has been very successful, this only allows measurements to be carried out up to 1.15 GeV per nucleon. To go higher at COSY we must work in inverse kinematics and use the polarised deuterium target in conjunction with a proton beam. The charge exchange can then be studied purely through the measurement of two slow protons in the silicon tracking telescopes without using the ANKE magnetic spectrometer at all. However, this opens even more fascinating possibilities, such as the study of Δ isobar production in $\vec{p}\vec{d} \to \{pp\}_s\Delta^0$, where the spin alignment of the Δ isobar can be determined through the measurement of one of the products of the $\Delta^0 \to p\pi^-$ decay. On the other hand, with its array of detectors, ANKE can investigate simultaneously a wide range of nuclear reactions, which makes the spin programme at the facility so exciting.

The work was partially supported by the COSY-FFE programme and by grants from the DFG (436 RUS 113/965/0-1) and GNSF (ST09-1024-4-200).

1. S. Barsov et al., Nucl. Instrum. Methods Phys. Res. A **462**, 364 (2001).
2. R. Engels et al., AIP Conf. Proc. **1149**, 890 (2009).
3. A. Kacharava, F. Rathmann, and C. Wilkin, COSY proposal #152 (2005), arXiv:nucl-ex/0511028.
4. A.Kacharava and C.Wilkin, Submitted to NUPECC, arXiv:nucl-ex/1212.2771.
5. D. Chiladze et al., Eur. Phys. J. A **40**, 23 (2009).
6. D. Mchedlishvili et al., submitted to Eur. Phys. A, arXiv:nucl-ex/1212.2365.
7. S.Yaschenko et al., Phys.Rev.Lett. **94**, 072304 (2005)
8. D. Tsirkov et al., Phys. Lett. B **712**, 370 (2012).
9. S. Dymov et al., Phys. Lett. B **712**, 375 (2012).
10. D. Tsirkov et al., FZ-Juelich IKP annual report 2010, available from `http://www2.fz-juelich.de/ikp/anke/en/`
11. T. Rausmann et al., COSY proposal # 157.1 (2007). This and other ANKE proposals are available from `www.fz-juelich.de/ikp/anke/en/proposals.shtml`.
12. P.Goslawski et al., Phys. Rev. ST-AB **13**, 022803 (2010).
13. P.Goslawski et al., Phys. Rev. D **85**, 112011 (2012).
14. S. Dymov, COSY proposal #192 (2008).
15. A. Kulikov, COSY proposal #158 (2008).
16. C. Hanhart, Phys. Rep. **397**, 155 (2004).

17. S. Dymov, COSY proposal #205 (2010).
18. R. Bilger et al., Nucl. Phys. A **693**, 633 (2001).
19. F. Duncan et al., Phys. Rev. Lett. **80**, 4390 (1998).
20. H. Hahn et al., Phys. Rev. C **53**, 1074 (1996).
21. H. Hahn et al., Phys. Rev. Lett. **82**, 2258 (1999).
22. K.Grigoryev et al., NIM A **599**, 130 (2009).
23. D. V. Bugg and C. Wilkin, Nucl. Phys. A **467**, 575 (1987).
24. J. Carbonell, M. B. Barbaro, and C. Wilkin, Nucl. Phys. A **529**, 653 (1991).
25. SAID data base, http://gwdac.phys.gwu.edu.
26. C. Ellegaard et al., Phys. Rev. Lett. **59**, 974 (1987).
27. S. Kox et al., Nucl. Phys. A **556**, 621 (1993).
28. D. Mchedlishvili, PoS (STORI'11), **040** (2011), `http://pos.sissa.it`.